Simulation of CHF using a Non-Heating Experimental Method Applying Ratio of Similitude

Hae-Kyun Park and Bum-Jin Chung*
Department of Nuclear Engineering, Kyung Hee University
#1732 Deogyeong-daero, Giheung-gu, Yongin-si, Gyeonggi-do, 17104, Korea
**Corresponding author: bjchung@khu.ac.kr*

1. Introduction

In the early study regarding CHF, Nukiyama [1] firstly identified the relationship between wall super heat and wall heat flux [2]. Because of the drastic rise of wall temperature after CHF point, the system failure may occur and thus the CHF is often conceived as the maximum manageable heat flux. Hence, numerous studies regarding CHF have been conducted over the last half a century [3-9] and several models and correlations predicting CHF value have been developed. Meanwhile the experimental investigation about CHF is difficult due to its extreme thermal condition near the CHF value (~ 1 MW/m^2).

In this paper the authors proposed a non-heating experimental method to simulate the CHF condition using mass transfer system by extending traditional copper-electroplating system. Hydrogen reduction phenomenon via electrochemical process substitutes vaporization in the boiling system. Copper electrode and 1.5 M of sulfuric acid aqueous solution was used as working surface and working fluid, respectively.

2. Existing CHF models

2.1. Hydrodynamic Instability Model

Kutateladze [3] developed the CHF correlation based on dimensional analysis in an incipient study. And then, Zuber [4] was inspired by Kutateladze's work and established CHF correlation applying to the Rayleigh-Taylor instability and Kelvin-Helmholtz instability as expressed in Eq. (1). Compared with the other experimental data, K value was determined as 0.131 for water boiling experiment.

$$q''_{CHF} = K h_{lg} \rho_g^{1/2} [\sigma g(\rho_l - \rho_g)]^{1/4} \tag{1}$$

2.2. Macrolayer Dryout Model

Haramura and Katto [5] proposed macrolayer dryout model. They succeeded Katto and Yokoya's study [6] and suggested that the CHF is related with presence of macrolayer. They postulated that the CHF occurs when the macrolayer is completely vaporized before the vapor mushroom departs from the heating surface. As a result, the CHF correlation was derived in terms of the liquid vaporization at the macrolayer.

$$\tau_d q''_{CHF} = \delta_l h_{lg} \rho_l (A_h - A_v) \tag{2}$$

τ_d, δ_l, A_h and A_v represents hovering period, thickness of macrolayer, heated area, and area of the vapor stem respectively. And the CHF correlation, Eq. (3) could be derived introducing Eq. (2).

$$q''_{CHF} = h_{lg} \rho_g^{0.5} [\sigma g(\rho_l - \rho_g)]^{1/4} (1+k)^{5/16} \left(\frac{\pi^4}{2^{11} \cdot 3^2}\right)^{1/16} \left(\frac{A_v}{A_w}\right)^{5/8} \left(1 - \frac{A_v}{A_w}\right)^{5/16} \left[\left(\frac{\rho_l}{\rho_g} + 1\right) / \left(\frac{11}{16}\frac{\rho_l}{\rho_g} + 1\right)^{3/5}\right]^{5/16}. \tag{3}$$

2.3. Dry Spot Model

Van Ouwerkerk [10] observed irreversible growth of dry areas at the pool boiling CHF condition using glass disk and n-heptane. Ha and No [11] proposed dry spot model and insisted that the critical number of bubbles surrounding an isolated bubble is five. Chung and No [12] established nucleate boiling limitation model which predicts CHF condition based on dry area fraction studied by Ha and No [11]. As a result, they proposed the heat flux prediction equation from nucleate boiling to a CHF expressed as following relation.

$$q = q_{nb}(n_{ib} / n_a) \tag{4}$$

where q_{nb}, n_{ib} and n_a represents nucleate boiling heat flux, number of isolated bubbles without coalescence and expected number of isolated bubbles, respectively.

3. Experiments

3.1. Methodology

Heat and mass transfer systems are analogous because their mathematical models describing the systems are identical [13]. Thus they can be treated applying similar structure of governing equations. Thus, the experimental technique using $CuSO_4$-H_2SO_4 electroplating system in the aspect of the analogy concept has been developed [14-16]. In this system the applied current between anode and cathode increases, the potential increases resulting in the evolution of hydrogen.

The basic idea of this methodology is that the CHF phenomenon due to the bubble behavior on the surface can be simulated through the evolution of hydrogen in mass transfer system. The authors assumed that if hydrogen generation rate exceeds a certain limit, the similar phenomenon with the CHF may occur on the cathode surface (Critical Current Density, CCD). Hydrogen generation rate can be calculated with Eq. (5).

$$\eta = V_m \left(\frac{T}{273.15} \right) \left(\frac{I}{neN_A} \right) \tag{5}$$

And hydrogen generation rate in the present work (m^3/s), η can be calculated by I, n, e and N_A, which represent current, number of the electron charge to reduction hydrogen ion, magnitude of the charge of an electron and Avogadro constant, respectively. And the molar volume of hydrogen (m^3/mole), V_m transforms molar generation of hydrogen into volume generation, which was dependent on the temperature with respect to the Charles's law. And then the applied heat flux is simulated as follows, Eq. (6).

$$q_{CHF} = \eta h_{fg} \rho_g \tag{6}$$

The products of η in Eq. (5) by present experiment, latent heat, h_{fg} and density of vapor, ρ_g transforms the applied current at CCD condition into the CHF condition in the heat transfer system.

3.2. Experimental Setup

3.2.1. Surface characteristics.

It is well known that the boiling phenomena including the CHF condition are strongly governed by surface characteristics such as wettability, roughness, porosity [17]. The authors measured each parameter to compare the result with boiling results that had identical surface condition. The measured contact angle, which related to surface wettability was 58° using sessile drop method. And surface roughness (R_a) and porosity was 20 nm and 8%, respectively. Thus the authors concluded that the surface characteristics of this experiment is similar with those of 'bare' and 'hydrophilic' surface condition.

3.2.2. Test apparatus.

The experimental apparatus and electric circuit are shown in Fig. 1. Copper disk of 10 mm diameter and diameter of 0.2 mm copper wire were located in a top-opened transparent tank at each experimental process. These cathodes simulate heating surface. And an anode copper plate is placed against the cathode to supply electric charges. The density and viscosity of 1.5 M of H_2SO_4 solution is 1097.3 kg/m^3 and 1.29×10^{-3} kg/m-s, respectively. The power supply (SGI 100A/150V, SGI) was used for potential control and Data Acquisition system (34972A, Agilent) was used for recording the data.

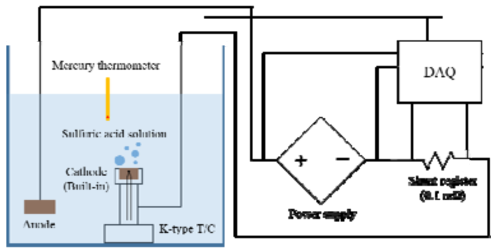

Fig. 1. Schematic design of the test electric circuit.

4. Results and discussion

4.1. Similarity in boiling curve

Figure 2 compares the typical boiling curve by Nukiyama [1] and the potential-current (V-I) curve using 10 mm copper disk. Potential increased as applied current increased, which shows similar trend to the nucleate boiling regime. However, the current does not increased over ~16 A despite of great potential. It seems that the vigorous coalescence of hydrogen at the cathode surface impeded supplement of the electron charge. The authors insisted that this phenomenon is similar to the CHF phenomenon, CCD (201.51 kA/m^2). This CCD can be transformed to CHF by using Eq. (5) and (6), 37.12 kW/m^2. This result is about 40 times smaller than that of the existing heat transfer results [5,8], which were implemented identical geometry condition with present works.

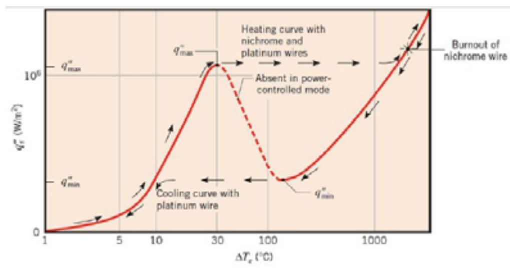

(a) Typical boiling curve [1]

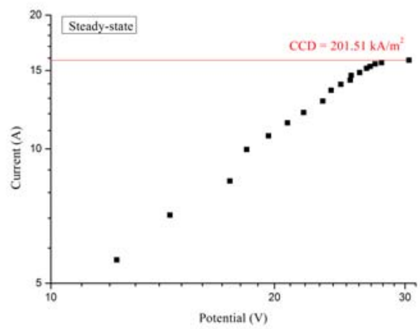

(b) CHF simulation results using mass transfer system.

Fig. 2. Comparison of the boiling and *V-I* curve.

4.2. Bubble behavior

Figure 3 compares photographic results of bubble behavior at CCD, CHF with hydrophilic surface and CHF with hydrophobic surface. The small sphere-shaped mushroom formed in the present work, as in the Fig. 3(a), while relatively large oval-shaped vapor mushroom formed at the heat transfer result of Ahn and Kim [8] as in the Fig. 4(b). Hence the CHF from present work had much small value compare to that of hydrophilic boiling results [5,8] in sketchy comparison. However, as shown in the Fig. 4(c), hydrogen mushroom behavior of the present work seems to be similar with heat transfer under hydrophobic surface condition. Although the surface wettability of the present work is hydrophilic, the authors postulated that the bubble behavior of the present system at CCD condition showed similar to that of hydrophobic system in the macroscopic point of view. The detailed analysis will provide following section.

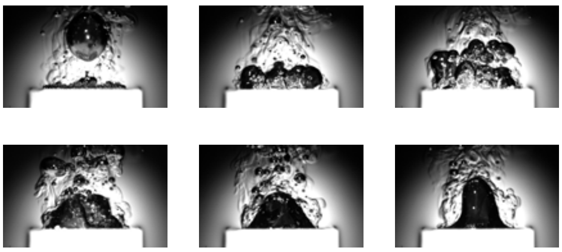

(a) Hydrogen mushroom behavior at CCD trigger.

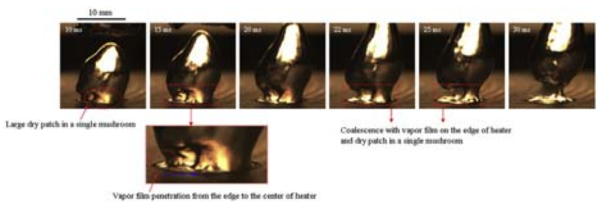

(b) Vapor mushroom behavior at CHF trigger [8].

(c) Vapor mushroom behavior of the heat transfer experiment with hydrophobic surface condition at CHF trigger [18].

Fig. 4. Photographs at CHF or CCD trigger.

4.3. Model Similarity

4.3.1. Nucleate bubble behavior.

In the boiling system, nucleate site density, n_a, bubble departure diameter, D_b, and bubble frequency, f are increase as heat flux increases generally. Chung and No's nucleate boiling limitation model [12] describes the CHF phenomenon based on fraction of n_a and n_{ib}. At a certain high heat flux, bubbles start to coalescence and form dry areas. In this regime, as isolated nucleate boiling site decreases, boiling heat transfer coefficient decreases. And further increase in heat flux, isolated nucleate boiling sites is limited by an agglomeration at just after a CHF.

However in the present electrochemical system, hydrogen reduction reaction occurs at higher potential than its reduction potential (~ -0.83 *V*). Thus, 'nucleate reduction site density' is relatively higher than that of the boiling system and size of hydrogen diameters are randomly distributed as shown in Fig. 5. Hence, hydrogen diameter and distribution at this very low current regime is quite different with boiling system.

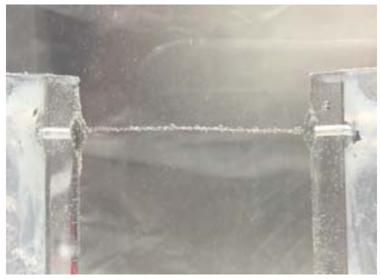

Fig. 5. Hydrogen behavior at 12 mA (Just after reduction potential).

Meanwhile at a certain higher current regime, hydrogen diameter and site density are generalized as shown in Fig. 6. Moreover, hydrogen diameter was increased as current increased, which is analogous with heat flux. Thus, the authors postulated that hydrogen behavior at this regime can simulate vapor bubble.

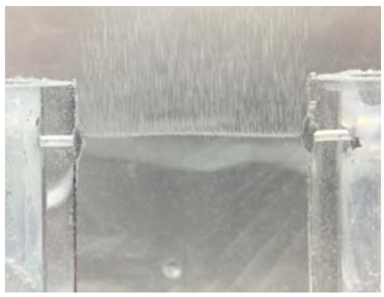

(a) Hydrogen behavior at 3 A.

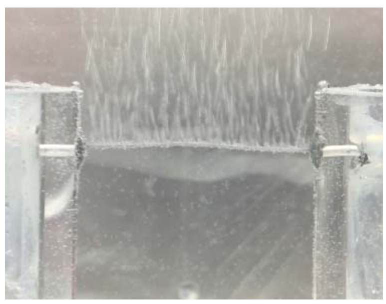

(b) Hydrogen behavior at 10 A.

Fig. 6. Hydrogen behavior that simulates vapor bubble.

4.3.2. Simulation of the CHF.

Based on the macroscopic observation, n_a and D_b of the present system are higher and smaller than those of water boiling system, respectively. If our system well agrees with nucleate boiling limitation model, the commence of the limitation in isolated nucleate boiling site occurs earlier than that of the water boiling system because of higher n_a. And this mechanism may yield earlier CHF as obtained in the present result.

If it is so, the present system may simulate 'downsize' of the water boiling system in terms of the 'similar figures' of the isolated bubble that just before forming agglomeration. And thus, it is possible that the CHF obtained from the present work can be corrected by the third power of bubble diameter ratio because the heat flux at the saturated boiling condition is governed by vapor volume generation rate.

4.4. Further Studies

In order to find correction factor for the CHF from the present work, more detailed and quantitative measurements of hydrogen bubble should be implemented. The authors will observe hydrogen behavior on the copper wire using high-speed camera measuring n_a, n_{ib}, D_b and bubble frequencies.

5. Conclusion

A non-heating experimental method to simulate the CHF is proposed. 1.5 M of sulfuric acid aqueous solution and the copper electrodes were employed to generate hydrogen at the cathode, which simulated vaporization phenomenon in the boiling system. Based on this motivation, CHF can be transformed by measuring critical current density. The obtained CHF from the present work is about 40 times smaller than the results of water boiling system.

The authors also observed nucleate hydrogen behavior and roughly compared with typical water boiling system. The n_a and D_b were higher and smaller than the water boiling system. Hence, the present system may simulate 'downsize' water boiling system in terms of 'similar figures' in bubble behaviors. Thus, using ratio of similitude in bubble diameter, the CHF from the present work could be corrected.

For more elaborated correction, more developed observation in hydrogen behaviors using high-speed camera should be implemented.

ACKNOWLEDGMENT

This work was supported by the National Research Foundation of Korea(NRF) grant funded by the Korea government(MSIT: Ministry of Science and ICT) (Grant code: 2017M2A8A4015283).

REFERENCES

[1] S. J. Nukiyama, The maximum and minimum values of the heat flux transmitted from metal to boiling water under atmospheric pressure, International Journal of Heat and Mass Transfer, Vol.9, pp. 1419-1433, 1966.

[2] Y. Koizumi, M. Shoji, M. Monde, Y. Takata, N. Nagai, "Boiling", Elsevier, Amsterdam, 2017.

[3] S.S. Kutateladze, A hydrodynamic model of the critical heat transfer in boiling liquids with free convection, Zhurn. Tekhc., Fiz., Vol.20, pp. 1389-1392, 1950.

[4] N. Zuber, Hydrodynamic aspects of boiling heat transfer, AEC Report No. AECU-4439, Physics and Mathematics, 1959.

[5] Y. Haramura and Y. Katto, A new hydrodynamic model of critical heat flux, applicable widely to both pool and forced convective boiling on submerged bodies in saturated liquids, International Journal of Heat and Mass Transfer, Vol.26, pp. 389-399, 1983.

[6] Y. Katto and S. Yokoya, Principal mechanism of boiling crisis in pool boiling, International Journal of Heat and Mass Transfer, Vol.11, pp. 993-1002, 1968.

[7] S.G. Kandlikar, A theoretical model to predict pool boiling CHF incorporating effects of contact angle and orientation, Journal of Heat Transfer, Vol.123, pp. 1071-1079, 2001.

[8] H.S. Ahn, M. H. Kim, Visualization study of critical heat flux mechanism on a small and horizontal copper heater, International Journal of Multiphase Flow, Vol.41, pp. 1-12, 2012.

[9] I.C. Bang, S. H. Chang, W. P. Beak, Visualization of a principle mechanism of critical heat flux in pool boiling, International Journal of Heat and Mass Transfer, Vol.48, pp. 5371-5385, 2005.

[10] H. J. Van Ouwerkerk, Burnout in pool boiling: the stability of boiling mechanisms, International Journal of Heat and Mass Transfer, Vol.15, pp.25-34, 1972.

[11] S. J. Ha, H. C. No, A dry-spot model of critical heat flux in pool and forced convection boiling, International Journal of Heat and Mass Transfer, Vol.41(2), pp. 303-311, 1998.

[12] H. J. Chung, H. C. No, A nucleate boiling limitation model for the prediction of pool boiling CHF, International Journal of Heat and Mass Transfer, Vol.50, pp. 2944-2951, 2007.

[13] F.P. Incropera, Foundation of Heat Transfer, John Wiley & Sons, New Yotk, pp. 622-638, 2012.

[14] E. J. Fenech and C. W. Tobias, Mass transfer by free convection at horizontal electrodes, Electrochimica Acta, Vol.2, pp. 311-325, 1960.

[15] S. H. Ko, D. W. Moon, B. J. Chung, Applications of electroplating method for heat transfer studies using analogy concept, Nuclear Engineering and Technology, Vol.38, pp. 251-258, 2006.

[16] B. J. Ko, W. J. Lee, B. J. Chung, Turbulent mixed convection heat transfer experiments in a vertical cylinder using analogy concept, Nuclear Engineering Design, Vol.240, pp. 3967-3973, 2010.

[17] H. O'Hanley, C. Coyle, J. Buongiorno, T. McKrell, L.W. Hu, M. Rubner, R. Cohen, Separate effects of surface roughness, wettability and porosity on the boiling critical heat flux, Applied Physics Letters, Vol.103(2), 024102, 2013.

[18] https://www.youtube.com/watch?v=hrvB1-dDqrA